Millimeter-wave arbitrary waveform generation with a direct space-to-time pulse shaper

J. D. McKinney, D. E. Leaird, and A. M. Weiner

School of Electrical and Computer Engineering, Purdue University, West Lafayette, Indiana 47907-1285

Received March 8, 2002

By using tailored pulse sequences from a novel, 1.5-μm direct space-to-time pulse shaper driving a high-speed photodetector, we have achieved, for the first time to our knowledge, millimeter-wave arbitrary waveform generation at center frequencies approaching 50 GHz. By appropriately designing the driving optical pulse sequences, we demonstrate the ability to synthesize strongly phase- and frequency-modulated millimeter-wave electrical signals on a cycle-by-cycle basis. © 2002 Optical Society of America

OCIS codes: 200.4560, 320.5540.

Fourier-transform (FT) optical pulse shaping[1] is now a well-established technology for generating nearly arbitrarily shaped ultrafast optical pulses, with applications ranging from coherent control to high-speed communications. Arbitrary waveform generation (AWG) capabilities for microwave and millimeter-wave (mm-wave) signals are, however, quite limited. Efficient mm-wave AWG could find application in ultrawide-bandwidth, secure, and multiple-access communication systems, in addition to electronic countermeasures and radar. Given the current limitations of commercial radio-frequency AWG instrumentation (current products can only simulate real-world signals up to ~2 GHz), the use of an ultrafast optical pulse train to drive a high-speed optical-to-electronic converter at multiple tens of gigahertz could dramatically improve the state of the art in microwave and mm-wave AWG. In previous work in our group, we used pulse sequences from a FT pulse shaper to drive a THz photoconductive antenna, resulting in generation of freely propagating phase- and amplitude-modulated THz radiation signals.[2] Another group recently demonstrated a phase-modulated waveform in the low- (~6-) GHz range by using a wavelength-division multiplexing technique combined with a series of optical delay lines to generate a driving pulse sequence.[3] Here we demonstrate, for the first time to our knowledge, mm-wave AWG at center frequencies up to ~50 GHz, effectively filling the void between the previous results. Our work utilizes a novel direct space-to-time (DST) pulse shaper,[4] which provides pulse shaping over a 100-ps temporal window, as required for waveform generation at tens of gigahertz. Additionally, by appropriately predistorting the driving optical waveforms from the DST shaper we are able to achieve amplitude equalization of the output mm-wave signals.

DST pulse shaping, originally demonstrated with picosecond pulses,[5] has been shown to be an effective method of generating high-bit-rate optical data packets.[6] The behavior of this apparatus in the femtosecond regime has been well analyzed,[4] and the ability to obtain multiple, temporally identical, waveforms at different center wavelengths and to control chirp has been demonstrated.[4,7] In contrast to the well-known FT pulse shaper, the temporal output of a DST shaper is a directly scaled version of the spatial profile of a spatially patterned femtosecond input beam. We previously demonstrated operation of a DST shaper, using femtosecond pulses at 850 nm from a Ti:sapphire laser.[4]

Here we use a DST pulse shaper constructed for the first time to operate in the 1.55-μm lightwave communications band. A schematic of our DST pulse shaper is shown in Fig. 1. The pulse shaper consists of a 600-line/mm diffraction grating and a 15-cm achromat lens. The pulse-shaper output is collected with a single-mode fiber, which acts as the output slit. Our previous work with DST pulse shaping relied on the use of an amplitude mask to generate the required spatial patterns.[4,6,7] Since the input spatial profile was equal to the amplitude mask pattern multiplied by the original Gaussian beam spatial profile, the output waveform was equal to a directly scaled version of the amplitude masking pattern multiplied by a Gaussian time aperture function. Here we address this problem by introducing a diffractive optical element[8] (DOE) to realize the required spatial patterning. This phase-only mask splits a single input beam into multiple, nearly equal intensity, spatial spots (8–21 with our DOEs), essentially without loss. This allows us to realize a significantly wider time aperture of up to $\gtrsim$100 ps, which is necessary for creation of radio-frequency waveforms with center frequencies in the range of multiple tens of gigahertz. Subsequent to the DOE, a separate spatial mask is used to further manipulate the periodic spatial patterns generated by

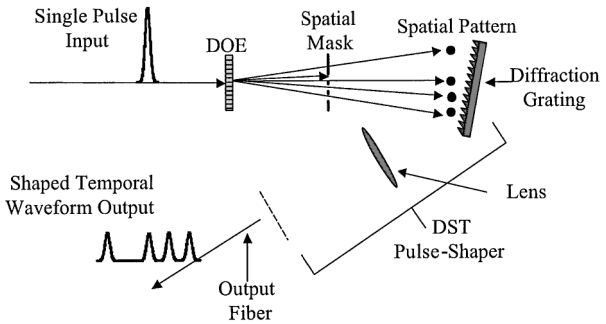

Fig. 1. 1.5-μm DST pulse shaper.

0146-9592/02/151345-03$15.00/0

the DOE. By appropriate tailoring of this mask, the period, spacing, position, and amplitude of spots in the spatial pattern can be adjusted. As a result of the space-to-time mapping, the output pulse sequences from the DST shaper are adjusted as well. It should be noted that the fixed mask used to manipulate the periodic pattern from the DOE could be replaced with a spatial light modulator, such as a liquid-crystal modulator, which is frequently used in FT pulse shapers. Inclusion of this programmable mask would allow the spatial input pattern to be altered via electronic control. Additional novel features of our DST shaper include operation with fiber input and output and the use of a grating with low polarization-dependent loss, which makes the DST pulse shaper insensitive to input polarization (this is important, since the polarization state is usually not preserved in fibers). A complete description of our 1.5-μm DST pulse shaper will be given in the future.

A block diagram of our experiments is shown in Fig. 2. The output from a 40-MHz repetition-rate, passively mode-locked femtosecond fiber laser[9] is spectrally filtered to yield ~300-fs pulses, passed through a fiber amplifier, and then directed to a DST pulse shaper, which generates tailored pulse sequences. These pulse sequences are then reamplified and directed onto a 60-GHz photodiode, resulting in shaped mm-wave signals, which are measured on a 50-GHz-bandwidth oscilloscope. In this method, formation of the mm-wave signals is mediated by the driving pulses and the limited frequency response of the optical-to-electronic converter and the electrical measurement system. By using pulses that are spaced too closely to be completely resolved by the electrical system, smooth mm-wave sinusoids can be created from pulsed optical waveforms. Examples of this are shown in Fig. 3. For these signals, spatial patterns corresponding to optical pulse sequences with periods of 20.8 ps (48 GHz) and 26.32 ps (38 GHz), after space-to-time conversion, were used as the input optical signals to our system. As is evident from Fig. 3, the measured signals show good agreement with 48- and 38-GHz sinusoids. Millimeter waveforms generated in our system exhibit peak-to-peak amplitudes of ~3 mV, as determined by the source laser power, the photodetector responsivity, and the electrical system response. To boost the amplitude for applications, either wideband electronic amplification or stronger optical excitation pulses will be needed.

We now present several compelling examples of mm-wave AWG. Figure 4 shows examples of phase modulation at 48 GHz. The top trace is the same 48-GHz sinusoidal burst as in Fig. 3(a). However, in the lower traces, the mm-wave waveforms contain a π phase shift, which occurs at different places within the waveform in the different traces. One can clearly see the phase shifts by comparing the positions of peaks and nulls between the top and lower waveforms. In these examples the mm-wave phase shift is induced by control of the timing of the optical pulses. For example, in the lowest trace, the optical pulses occur at approximately −60, −40, −20, 0, 30, and 50 ps. The additional ~10-ps extra delay between the fourth and fifth pulses yields the π phase shift. This result clearly illustrates how controlling the temporal position of pulses in the driving optical pulse sequence makes phase modulation of the output electrical waveform possible.

Figure 5 shows an example of frequency modulation. The first cycles of the waveform occur at 48 GHz, which then changes abruptly to 24 GHz for the last two cycles. Here the frequency modulation is controlled by variation of the repetition rate of the

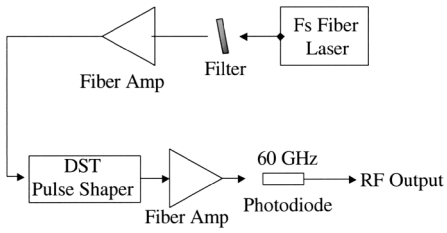

Fig. 2. Schematic diagram of the experimental setup. Fs, femtosecond; RF, radio-frequency.

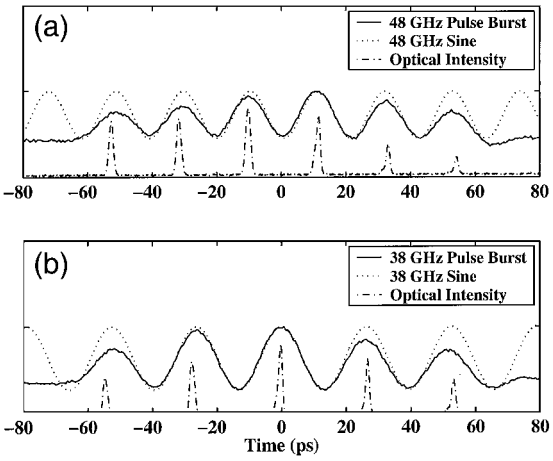

Fig. 3. (a) 48-GHz mm-wave burst, (b) 38 GHz mm-wave burst. The mm-wave signals can be seen to be good sinusoids, in contrast to the optical pulse sequences driving the photodiode (bottom traces).

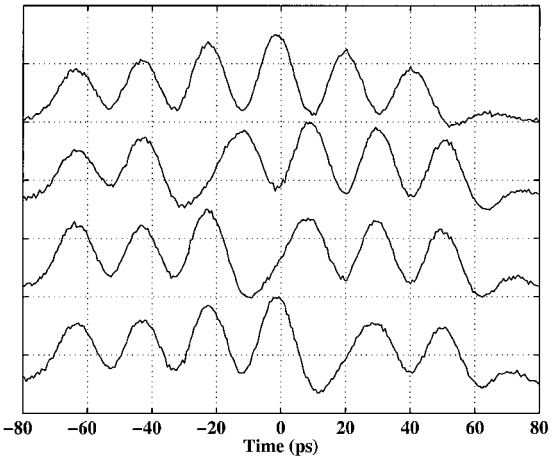

Fig. 4. Example of mm-wave phase modulation. The phase of the mm-wave waveform can be adjusted by changes in the relative timing of pulses in the driving optical waveform.

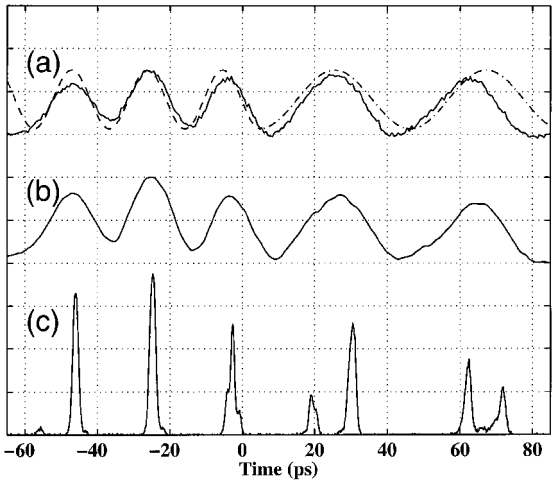

Fig. 5. Example of mm-wave frequency modulation. (a) mm-wave data and 48- and 24-GHz sinusoidal fits. (b) Predicted mm-wave data based on the convolution of the driving optical waveform and the electrical system's impulse response. (c) Cross-correlation measurement of the driving optical waveform.

driving optical pulse sequence in concert with the electrical bandwidth limitations. In particular, the trick to obtaining the lower frequency is to use pulse pairs spaced too closely (~10 ps) to be resolved by the electrical system. The responses from each of the pulses in the pair smear together, yielding a single mm-wave cycle that is twice as long as for single-pulse excitation. Good agreement was found between the measured mm-waveform and the 48- and 24-GHz sinusoidal fits, as shown in the top traces of Fig. 5. In addition, when the measured optical cross correlation is convolved with the electrical measurement system's impulse response, the resulting predicted mm-wave waveform agrees quite well with the measured waveform, as illustrated in Fig. 5. It is apparent from the optical cross correlation (bottom trace of Fig. 5) that the pulse pairs driving the 24-GHz portion of the electrical waveform are lower in amplitude than the single pulses driving the 48-GHz electrical signal. We observe that, when these pulse pairs were of the same amplitude as the pulses driving the 48-GHz cycles, the lower-frequency cycles of the millimeter waveform were larger in amplitude than the preceding cycles. This is due in part to the electrical system, which has a greater response at 24 GHz. We purposely attenuated the pulse pairs shown in Fig. 5 to equalize the intensity of the electrical waveform. In this manner we are able to achieve equalization of the output electrical waveform by intentionally predistorting the input optical pulse sequence to compensate for the electrical system's frequency response. This example clearly illustrates cycle-by-cycle mm-wave waveform synthesis.

We are currently limited to burst millimeter waveforms, which at most fill the temporal window (~100 ps) of our DST shaper. The waveforms are temporally isolated and repeat at the 25-ns repetition rate of our source laser. This work could be extended by use of a higher-repetition-rate source, e.g., at 10 GHz, which would permit generation of continuously repetitive mm-wave signals with an essentially arbitrary user-defined structure within one repetition period.

In summary, we have exploited optical pulse-shaping technology to demonstrate mm-wave arbitrary waveform generation up to ~50 GHz. By controlling the amplitude, pulse-to-pulse spacing, and repetition rate of the driving optical pulse sequence, we are able to obtain equalized mm-wave waveforms exhibiting arbitrary phase and frequency modulation.

This material is based on work supported by or in part by the U.S. Army Research Office under contract DAAD19-00-0497 and the National Science Foundation under grant 0100949-ECS and by Tektronix. J. D. McKinney's e-mail address is mckinnjd@ecn.purdue.edu.

References

1. A. M. Weiner, Rev. Sci. Instrum. **71,** 1929 (2000).
2. Y. Liu, S.-G. Park, and A. M. Weiner, IEEE J. Sel. Top. Quant. Electron. **2,** 709 (1996).
3. B. Jalali, P. Kelkar, and V. Saxena, in *Proceedings of the 14th Annual Meeting of the IEEE* (IEEE Lasers and Electro-Optics Society, Piscataway, N.J., 2001), pp. 253–254.
4. D. E. Leaird and A. M. Weiner, IEEE J. Quantum Electron. **37,** 494 (2001).
5. Ph. Emplit, J. P. Hamaide, and F. Reynaud, Opt. Lett. **17,** 1358 (1992).
6. D. E. Leaird and A. M. Weiner, Opt. Lett. **24,** 853 (1999).
7. D. E. Leaird and A. M. Weiner, Opt. Lett. **25,** 850 (2000).
8. J. N. Mait, J. Opt. Soc. Am. A **7,** 1514 (1990).
9. K. Tamura, H. A. Haus, and E. P. Ippen, Electron. Lett. **28,** 2226 (1992).